

**Preformed Cooper pairs in flat-band semimetals**Alexander A. Zyuzin<sup>1</sup> and A. Yu. Zyuzin<sup>2</sup><sup>1</sup>*Department of Applied Physics, Aalto University, FI-00076 AALTO, Finland*<sup>2</sup>*Ioffe Physical-Technical Institute, 194021 St. Petersburg, Russia*

(Received 8 October 2021; accepted 6 July 2022; published 19 July 2022)

We study conditions for the emergence of the preformed Cooper pairs in materials hosting flat bands. As a particular example, we consider a semimetal, with a pair of three-band crossing points at which a flat band intersects with a Dirac cone, and focus on the *s*-wave intervalley pairing channel. The nearly dispersionless nature of the flat band at strong attraction between electrons promotes local Cooper pair formation so that the system may be modeled as an array of superconducting grains. Due to dispersive bands, Andreev scattering between the grains gives rise to the global phase-coherent superconductivity at low temperatures. We develop a mean-field theory to calculate transition temperature between the preformed Cooper pair state and the phase-coherent state for different interaction strengths in the Cooper channel. The transition temperature between semimetal and preformed Cooper pair phases is proportional to the interaction constant, the dependence of the transition temperature to the phase-coherent state on the interaction constant is weaker.

DOI: [10.1103/PhysRevB.106.L020502](https://doi.org/10.1103/PhysRevB.106.L020502)

In condensed-matter systems the nearly dispersionless flat-band electronic structure may stimulate the interaction-induced instabilities. Of particular interest is the interplay between flat band and superconductivity. The reason for that is the relatively large value of the superconducting transition temperature, which can be linearly proportional to the pairing interaction strength as was proposed by Khodel' and Shaginyan [1] and later studied for instance in Refs. [2–7].

The examples of flat-band systems include multilayer graphene with rhombohedral stacking [4], interfaces between the domains in graphene with Bernal stacking order [8], twisted bilayer graphene [9,10], and semimetals with integer pseudospin quasiparticles [11–13]. The latter is characterized by the existence of multiple-band crossing points at which the flat band intersects with the Dirac cones. For example, the low-energy electron excitations can be described by the Hamiltonian for a pseudospin-one particle, see Ref. [13].

Recently superconductivity has been observed in twisted bilayer graphene [14] and in Bernal bilayer graphene subject to applied perpendicular electric field [15]. Signatures of superconductivity have been observed in highly oriented pyrolytic graphite [8,16]. Although, the semimetals hosting three-band touching points (and among them CoSi and RhSi) have been discovered [17–19] (see Ref. [20] for a review) and several flat-band enhanced Cooper pairing channels have been explored theoretically [5,21], superconductivity has not been detected yet. Despite intensive research, the role of flat band in the Cooper pairing is far from being understood [16].

We emphasize that the effect of the flat band on the formation of superconductivity can be twofold. On one hand, the strong enhancement of the electronic density of states leads to higher critical temperatures of Cooper pairing. On the other, its nearly dispersionless nature can be a serious impediment to pair condensation. The flat band favors the localization of quasiparticles, which suppresses the superconducting phase

stiffness. It works against the long-range coherence leading rather to a situation with preformed Cooper pairing [22].

The problem of flat-band induced correlations between the Cooper pairs was analysed in Ref. [23]. The flat-band contribution to superconducting phase stiffness was shown to be finite and originate from the position-dependent matrix structure of the respective wave function. It is now believed that this contribution might eventually support the pair condensation. However, we argue that Ref. [23] overlooks superconductivity and deals with the preformed Cooper pair phase and the properties of the local pairs. In this theory, the flat-band contribution to phase stiffness results in narrow-range spatial correlations on the scale of the size of the preformed Cooper pair itself. Instead, we expect different situation, in which local Cooper pairs coexist with the Fermi liquid.

In our context, however, the Cooper pair formation and their condensation occur at different temperatures [24,25]. In contrast to the previous research [1–7], we emphasize the importance of both localized and delocalized quasiparticles on the emergence of superconductivity. In addition to the flat band, materials inevitably host dispersive bands as well, which essentially contribute to the pair condensation. Such situation exists in considered three-band semimetal. We note that our theory might be extended to explain superconductivity in bilayer graphene with twisted and Bernal stacking.

We show that with the increase of electron-electron attraction, the system reaches a state, which can be modeled by an emergent granularity. It can be described by the Cooper pairs localized inside the grains lacking the long-range coherence. The superconducting order parameter exhibits strong spatial fluctuations. The long-ranged Andreev coupling between the grains, thanks to the contribution of dispersive bands, establishes a coherent state at a lower temperature. We develop

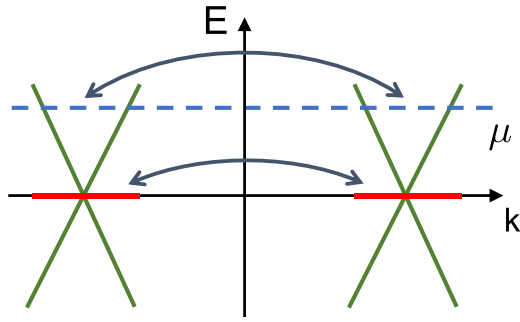


FIG. 1. Schematics of the band structure  $E(\mathbf{k})$  in the vicinity of two three-band-touching points at chemical potential  $\mu$ . There are two points at which Dirac cones and flat bands intersect. Superconducting pairing of electrons from different valleys is considered.

a mean-field theory to calculate the temperatures of Cooper pairs formation and their consecutive condensation.

*Model of semimetal.* We consider a time-reversal symmetric semimetal with a pair of three-band crossing points at momenta  $\pm\mathbf{K}_D$  in the first Brillouin zone as shown schematically in Fig. 1. As we ignore the single-particle intervalley scattering processes, the model Hamiltonian can be represented via a sum of two independent contributions from two valleys [13]:  $\mathcal{H} = \int_{\mathbf{k}} \sum_{s=\pm} \Psi_{s,\mathbf{k}}^\dagger v_F \mathbf{S} \cdot \mathbf{k} \Psi_{s,\mathbf{k}}$ , where  $v_F$  is the Fermi velocity,  $\mathbf{k}$  is the momentum measured relatively to the  $\pm\mathbf{K}_D$  with  $k \ll K_D$ ,  $\int_{\mathbf{k}}(\dots) \equiv \int \frac{d\mathbf{k}}{(2\pi)^3}(\dots)$ , and  $\mathbf{S} = (S_x, S_y, S_z)$  are the Gell-Mann matrices acting on “which band” pseudospin degree of freedom; see the Supplemental Material [26]. The electron operators are defined by  $\Psi_{s,\mathbf{k}} = [\Psi_{s,+1,\mathbf{k}}, \Psi_{s,0,\mathbf{k}}, \Psi_{s,-1,\mathbf{k}}]^T$ , where indices  $\pm 1, 0$  correspond to three different bands, two of which are dispersive,  $E_{\pm 1} = \pm v_F k$ , and another is flat,  $E_0 = 0$ . The latter is considered in the infinite mass limit approximation, so that higher order momentum corrections are neglected. We will be using  $\hbar = k_B = 1$  units throughout the paper.

To analyze superconducting instability in the system, we introduce electron Green’s function in Matsubara representation  $G(\mathbf{r}, i\omega) = \int_{\mathbf{k}} G(\mathbf{k}, i\omega) e^{i\mathbf{k}\cdot\mathbf{r}}$ , where  $\omega = (2n+1)\pi T$  is the Matsubara frequency at temperature  $T$ . The Green’s function  $G(\mathbf{k}, i\omega) = (i\omega - v_F \mathbf{S} \cdot \mathbf{k} + \mu)^{-1}$  can be expressed as [26]

$$G(\mathbf{k}, i\omega) = \frac{1 - (\mathbf{S}\mathbf{n}_k)^2}{i\omega + \mu} + \frac{1}{2} \sum_{s=\pm 1} \frac{(\mathbf{S}\mathbf{n}_k)^2 + s(\mathbf{S}\mathbf{n}_k)}{i\omega + \mu - sv_F k}, \quad (1)$$

where  $\mu$  is the chemical potential and  $\mathbf{n}_k = \mathbf{k}/k$  is a unit vector in the direction of momentum. The chemical potential can be positive or negative, although we choose it to be positive since it does not change our result. Attention shall be paid to the case of finite flat-band dispersion corrections, which violate the particle-hole symmetry [5]. We will comment on that later in the conclusions.

The first and second terms in (1) describe contributions of the flat and dispersive bands, which can be separated into the local and nonlocal terms as  $G(\mathbf{r}, i\omega) = G_{\text{loc}}(\mathbf{r}, i\omega) + G_{\text{nl}}(\mathbf{r}, i\omega)$ , respectively. The local contribution is given by

$$G_{\text{loc}}(\mathbf{r}, i\omega) = \frac{1}{i\omega + \mu} \left\{ \delta(\mathbf{r}) + \frac{1}{4\pi r^3} [3(\mathbf{S}\mathbf{n}_r)^2 - \mathbf{S}^2] \right\}, \quad (2)$$

where now  $\mathbf{n}_r = \mathbf{r}/r$  is the unit vector in coordinate space and  $\delta(\mathbf{r})$  is the Dirac delta function in three dimension. The second dipole-like term decays as a cube of distance smearing the delta function. In the limit of  $r \rightarrow 0$  the Green’s function is cut by the interatomic distance. We also note that the spatial and frequency dependent parts are separated in the flat-band model in the infinite mass approximation.

It suffices to consider the nonlocal term in the limiting case, where  $\mu \gg |\omega|$  and  $\mu r/v_F \gg 1$ ,

$$G_{\text{nl}}(\mathbf{r}, i\omega) = -\frac{\mu(\mathbf{S}\mathbf{n}_r)}{4\pi v_F^2 r} [\text{sgn}\omega + (\mathbf{S}\mathbf{n}_r)] e^{-\frac{r}{v_F}(\omega - i\mu)\text{sgn}\omega}. \quad (3)$$

The expected three-dimensional spatial coordinate dependence is supplemented by the unusual matrix structure. Let us now discuss superconductivity in flat-band semimetal.

*Model of superconductivity.* We consider  $s$ -wave superconducting instability in the flat-band semimetal taking three-band semimetal as a particular example [5]. However, we note that our results are generally valid for systems with coexisting dispersive and nearly flat bands. The symmetry analysis of the superconducting channels in three-band semimetal was performed in Refs. [5,21]. Specifically, for clean systems possessing time-reversal symmetry, it was found that the flat band enhances intervalley Cooper pairing with total pseudospin  $S = 0$ . The intervalley contribution to the interaction between electrons is given by [26]

$$U = -\lambda \sum_{\alpha,\beta} \int_{\mathbf{k},\mathbf{k}'} (\Psi_{1,\alpha,\mathbf{k}}^\dagger \Psi_{1,\alpha,\mathbf{k}'}) (\Psi_{-1,\beta,-\mathbf{k}}^\dagger \Psi_{-1,\beta,-\mathbf{k}'}), \quad (4)$$

where  $\lambda > 0$  is the interaction constant. We seek for the case in which flat-band significantly contributes to superconductivity. Among many possible superconducting states we focus on the  $s$ -wave intervalley odd pairing [5,21]. The pairing channels can be distinguished by the total pseudospin  $S$  of Cooper pairs. In our case, one can only have even  $S = 0$  and  $S = 2$  due to the Pauli principle. We focus on the  $S = 0$  channel, which has the highest superconducting transition temperature. The extended analysis of superconducting states for  $S = 2$  in the model, which takes into account quadratic momentum corrections to the single-particle Hamiltonian, can be found in [27].

Let us now qualitatively estimate the superconducting vertex part describing Cooper instability,

$$\det[1 - \lambda\Pi(\mathbf{q})] = 0, \quad (5)$$

where  $\Pi(\mathbf{q}) = T \sum_{\omega} \int_{\mathbf{k}} G(\mathbf{k}, i\omega) [G(\mathbf{q} - \mathbf{k}, -i\omega)]_{S \rightarrow -S}$  and summation is performed over the Matsubara frequencies. Due to the local term in Green’s function (2), the integrand in  $\Pi(\mathbf{q})$  diverges at large wave vectors. And it is convenient to single out nonlocal contributions (3), which contain the usual logarithmic ultraviolet cutoff. All in all, we separate local and nonlocal contributions  $\Pi(\mathbf{q}) = \Pi_{\text{loc}}(\mathbf{q}) + \Pi_{\text{nl}}(\mathbf{q})$  and neglect crossed terms between them (as we are interested in the two limiting cases only).

Consider momentum expansion of the vertex part  $\Pi(\mathbf{q}) \approx \Pi + q^2 \delta\Pi$ , where the second term describes superconducting stiffness. The contribution of the local term in Green’s function (2) to the superconducting vertex part  $\Pi_{\text{loc}} \sim (K^3/\mu)\text{th}(\mu/2T)$  is proportional to the volume of the flat band



low-doping case  $\mu \ll T$  requires large interaction constant  $\lambda/\lambda_c \gg 1$  for the transition. Here the critical temperature is proportional to the interaction constant and inversely proportional to the volume of preformed Cooper pair  $T_p = \lambda K^3/12$  [3–6].

At high doping  $\mu \gg T$ , the transition takes place when the interaction constant is larger than the critical value  $\lambda \simeq \lambda_c$  [24]. In this limit the coefficients in (9) can be simplified as  $a = 3(\lambda^{-1} - \lambda_c^{-1})$  and  $b = 3/(2\mu^2\lambda_c)$ . We shall focus on this case in what follows. Let us now calculate the transition temperature to the phase-coherent state, which is driven by the Andreev coupling.

*Transition between preformed-pair and phase-coherent states.* With the increase of interaction constant  $\lambda$ , the impact of dispersive bands enhances Andreev coupling between the superconducting grains. As a result, the system may reach the phase coherence. In what follows, we develop a mean-field theory to calculate the superconducting transition temperature.

Within the mean-field approach, the fluctuating values of the order parameter  $\Delta_i$  are replaced by an average order parameter  $\langle \Delta \rangle$  [25,26]. The self-consistent mean-field equation is

$$\langle \Delta \rangle = \frac{\int \mathcal{D}\Delta \mathcal{D}\Delta^* \Delta_0 e^{-F/T}}{\int \mathcal{D}\Delta \mathcal{D}\Delta^* e^{-F/T}} \approx \frac{\int d\Delta d\Delta^* \Delta e^{-F_{MF}/T}}{\int d\Delta d\Delta^* e^{-F_{MF}/T}}, \quad (10)$$

in which  $\mathcal{D}\Delta \equiv \prod_i d\Delta_i$ . The mean-field functional reads

$$F_{MF} = F_0 - \sum_{i \neq 0} F_{i,0} \\ = V_G \left[ a|\Delta|^2 + \frac{b}{2}|\Delta|^4 - c(\langle \Delta \rangle \Delta^* + \langle \Delta^* \rangle \Delta) \right]. \quad (11)$$

In the continuum limit, we substitute  $\sum_{i \neq 0} = V_G^{-1} \int_V d\mathbf{r}$  and obtain coefficient  $c = v_{nl} \ln |\mu/T|$  within the logarithmic accuracy.

Without losing the generality, the averaged order parameter  $\langle \Delta \rangle$  can be restricted to real value. At  $c(\Delta) \ll \sqrt{|a|T/V_G} \max(1, bT/a^2V_G)$ , expanding integrands in Eq. (10) in powers of  $\langle \Delta \rangle$ , we obtain

$$1 = v_{nl} \frac{V_G \langle |\Delta|^2 \rangle}{T} \ln \left| \frac{\mu}{T} \right|, \quad \langle |\Delta|^2 \rangle = \frac{\int_0^\infty dx x e^{-\frac{V_G}{T}(ax + \frac{b}{2}x^2)}}{\int_0^\infty dx e^{-\frac{V_G}{T}(ax + \frac{b}{2}x^2)}}. \quad (12)$$

The solution to Eq. (12) is shown in Fig. 2. Analytical expressions can be analysed in several limiting cases.

First, consider a situation in which the interaction constant  $\lambda$  is much smaller the critical value,  $\lambda \ll \lambda_c$ , so that  $\Delta_i = 0$  ( $a > 0$ ). In this weak-coupling regime, the  $bx^2$  term in formula (12) can be neglected provided  $a^2V_G/bT \gg 1$ . Performing integration in (12) one obtains expression for the square of quasiparticle energy gap  $\langle |\Delta|^2 \rangle \approx T/aV_G$ . As a result, the transition temperature to the coherent state is given by

$$T_c = \mu \exp \left\{ -\frac{3}{\lambda v_{nl}} (1 - \lambda/\lambda_c) \right\}. \quad (13)$$

This mean-field solution coincides with the exact BCS expression. The flat band gives  $1 - \lambda/\lambda_c$  enhancement correction in the exponent.

Second, consider a semimetal at the vicinity of the transition to preformed Cooper pair phase,  $\lambda \approx \lambda_c$ . At  $a^2V_G/bT \ll 1$ , we can neglect  $a$  term compared with the nonlinear  $b$  term in (12) and obtain  $\langle |\Delta|^2 \rangle \approx \sqrt{2T/\pi bV_G}$ . Taking into account  $V_G K^3 \approx 1$  and using expressions for  $\lambda_c$  and  $b$ , we find

$$T_c = \frac{2\mu}{9\pi} (\lambda_c v_{nl} \ln |\mu/T_c|)^2. \quad (14)$$

This result is valid for both signs of the coefficient  $a$ . Due to  $\lambda_c v_{nl} < 1$ , the  $T_c$  is proportional to the critical value of the interaction constant squared.

Third, consider the preformed Cooper pair phase,  $\lambda \gtrsim \lambda_c$ . For weak fluctuations  $a^2V_G/bT \gg 1$ , using  $\langle |\Delta|^2 \rangle \approx -a/b = 2\mu^2(1 - \lambda_c/\lambda)$ , we obtain

$$T_c = \frac{\lambda_c v_{nl}}{3} \mu \left( 1 - \frac{\lambda_c}{\lambda} \right) \ln \left| \frac{\mu}{T_c} \right|. \quad (15)$$

The transition temperature increases with the increase of  $\lambda$ . However, in the limit of  $\lambda \gg \lambda_c$ , the GL expansion is no longer valid. The investigation of this case deserves a separate study.

*Conclusions.* Let us now briefly comment on the effect of finite  $\propto k^2$  corrections to the Hamiltonian of semimetal. In this case, the flat band acquires a finite curvature. As noted in Ref. [5] accounting for such term results in vanishing of the threshold value  $\lambda_c$ , which is required for preformed Cooper pairing, provided the chemical potential crosses the band. Hence, enhancement of the transition temperature  $T_c$  (13) at smaller values of the interaction constant  $\lambda \rightarrow 0$  is expected for particular doping, which depends on the sign of  $\propto k^2$  correction term. We also note that materials may contain other dispersive bands, which can coexist with the Dirac cones at the chemical potential, and contribute to the long-range coupling as well.

It would be interesting to extend the above-presented research to explain superconductivity in twisted bilayer graphene [14] and in graphite with Bernal stacking order [8]. The moiré pattern can be modeled as a system of coupled grains [29]. We argue that in this situation the intergrain coupling leads to the phase-coherent state at temperatures lower than the temperature of the on-grain Cooper pair formation. We will consider superconductivity in twisted bilayer graphene in future work.

To conclude, in this paper we have demonstrated that a nearly dispersionless flat band at strong attraction between electrons manifests itself in the emergent granularity and the Cooper pair preformation. The dispersive bands, which coexist with the flat bands, promote the global phase-coherent superconducting state at low temperatures. We have calculated the temperature of the phase transition between the preformed pairs and phase-coherent states in a semimetal hosting a pair of three-band crossing points. Experimentally, the preformed Cooper pairs may be probed locally via low-temperature spectroscopy [22].

The authors are thankful to Vladimir Zyuzin for critical discussions and to Pirinem School of Theoretical Physics for warm hospitality. This research was supported by the

Academy of Finland (Project No. 308339) and in parts by the Academy of Finland Centre of Excellence program (Project No. 336810).

- 
- [1] V. A. Khodel' and V. R. Shaginyan, Superfluidity in system with fermion condensate, *Pis'ma Zh. Eksp. Teor. Fiz.* **51**, 488 (1990) [*JETP Lett.* **51**, 553 (1990)].
- [2] M. Imada and M. Kohno, Superconductivity from Flat Dispersion Designed in Doped Mott Insulators, *Phys. Rev. Lett.* **84**, 143 (2000).
- [3] S. Miyahara, S. Kusuta, and N. Furukawa, BCS theory on a flat band lattice, *Physica C: Superconductivity* **460-462**, 1145 (2007).
- [4] N. B. Kopnin, T. T. Heikkilä, and G. E. Volovik, High-temperature surface superconductivity in topological flat-band systems, *Phys. Rev. B* **83**, 220503(R) (2011).
- [5] Yu-Ping Lin and R. M. Nandkishore, Exotic superconductivity with enhanced energy scales in materials with three band crossings, *Phys. Rev. B* **97**, 134521 (2018).
- [6] T. J. Peltonen, R. Ojajarvi, and T. T. Heikkilä, Mean-field theory for superconductivity in twisted bilayer graphene, *Phys. Rev. B* **98**, 220504(R) (2018).
- [7] F. Wu, A. H. MacDonald, and I. Martin, Theory of Phonon-Mediated Superconductivity in Twisted Bilayer Graphene, *Phys. Rev. Lett.* **121**, 257001 (2018).
- [8] P. Esquinazi, T. T. Heikkilä, Y. V. Lysogorskiy, D. A. Tayurskii, and G. E. Volovik, On the superconductivity of graphite interfaces, *JETP Lett.* **100**, 336 (2014).
- [9] J. M. B. Lopes dos Santos, N. M. R. Peres, and A. H. Castro Neto, Graphene Bilayer with a Twist: Electronic Structure, *Phys. Rev. Lett.* **99**, 256802 (2007).
- [10] R. Bistritzer and A. H. MacDonald, Moiré bands in twisted double-layer graphene, *Proc. Natl. Acad. Sci. USA* **108**, 12233 (2011).
- [11] B. Dóra, J. Kailasvuori, and R. Moessner, Lattice generalization of the Dirac equation to general spin and the role of the flat band, *Phys. Rev. B* **84**, 195422 (2011).
- [12] J. L. Mañes, Existence of bulk chiral fermions and crystal symmetry, *Phys. Rev. B* **85**, 155118 (2012).
- [13] B. Bradlyn, J. Cano, Z. Wang, M. G. Vergniory, C. Felser, R. J. Cava, and B. A. Bernevig, Beyond Dirac and Weyl fermions: Unconventional quasiparticles in conventional crystals, *Science* **353**, aaf5037 (2016).
- [14] Y. Cao, V. Fatemi, S. Fang, K. Watanabe, T. Taniguchi, E. Kaxiras, and P. Jarillo-Herrero, Unconventional superconductivity in magic-angle graphene superlattices, *Nature (London)* **556**, 43 (2018).
- [15] H. Zhou, L. Holleis, Y. Saito, L. Cohen, W. Huynh, C. L. Patterson, F. Yang, T. Taniguchi, K. Watanabe, and A. F. Young, Isospin magnetism and spin-triplet superconductivity in Bernal bilayer graphene, *Science* **375**, 774 (2022)
- [16] G.E. Volovik, Graphite, graphene, and the flat band superconductivity, *JETP Lett.* **107**, 516 (2018).
- [17] D. Takane, Z. Wang, S. Souma, K. Nakayama, T. Nakamura, H. Oinuma, Y. Nakata, H. Iwasawa, C. Cacho, T. Kim, K. Horiba, H. Kumigashira, T. Takahashi, Y. Ando, and T. Sato, Observation of Chiral Fermions with a Large Topological Charge and Associated Fermi-Arc Surface States in CoSi, *Phys. Rev. Lett.* **122**, 076402 (2019).
- [18] Z. Rao, H. Li, T. Zhang, S. Tian, C. Li, B. Fu, C. Tang, L. Wang, Z. Li, W. Fan *et al.*, Topological chiral crystals with helicoid-arc quantum states, *Nature (London)* **567**, 496 (2019).
- [19] D. S. Sanchez, I. Belopolski, T. A. Cochran, X. Xu, J.-X. Yin, G. Chang, W. Xie, K. Manna, V. Süß, C.-Y. Huang *et al.*, Topological chiral crystals with helicoid-arc quantum states, *Nature (London)* **567**, 500 (2019).
- [20] B. Q. Lv, T. Qian, and H. Ding, Experimental perspective on three-dimensional topological semimetals, *Rev. Mod. Phys.* **93**, 025002 (2021).
- [21] Y.-P. Lin, Chiral flat band superconductivity from symmetry-protected three-band crossings, *Phys. Rev. Research* **2**, 043209 (2020).
- [22] B. Sacépé, M. Feigel'man, and T. M. Klapwijk, Quantum breakdown of superconductivity in low-dimensional materials, *Nat. Phys.* **16**, 734 (2020).
- [23] S. Peotta and P. Törmä, Superfluidity in topologically nontrivial flat bands, *Nat. Commun.* **6**, 8944 (2015).
- [24] P. Nozières and S. Schmitt-Rink, Bose condensation in an attractive fermion gas: From weak to strong coupling superconductivity, *J. Low Temp. Phys.* **59**, 195 (1985).
- [25] A. Yu. Zyuzin, Superconductivity in dilute system of sites with strong electron-electron attraction, [arXiv:2012.12597](https://arxiv.org/abs/2012.12597).
- [26] See Supplemental Material at <http://link.aps.org/supplemental/10.1103/PhysRevB.106.L020502> for Green's function, interaction in the Cooper channel, and mean-field theory for the transition between preformed-pair and phase-coherent states.
- [27] S. Mandal, J. M. Link, and I. F. Herbut, Time-reversal symmetry breaking and *d*-wave superconductivity of triple-point fermions, *Phys. Rev. B* **104**, 134512 (2021).
- [28] A. A. Abrikosov, L. P. Gorkov, and I. E. Dzyaloshinski, *Methods of Quantum Field Theory in Statistical Physics* (Dover Publications, New York, 1975) Ch. 7, Sec. 38.
- [29] Z.-D. Song and B. A. Bernevig, MATBG as topological heavy fermion: I. Exact mapping and correlated insulators, [arXiv:2111.05865](https://arxiv.org/abs/2111.05865).